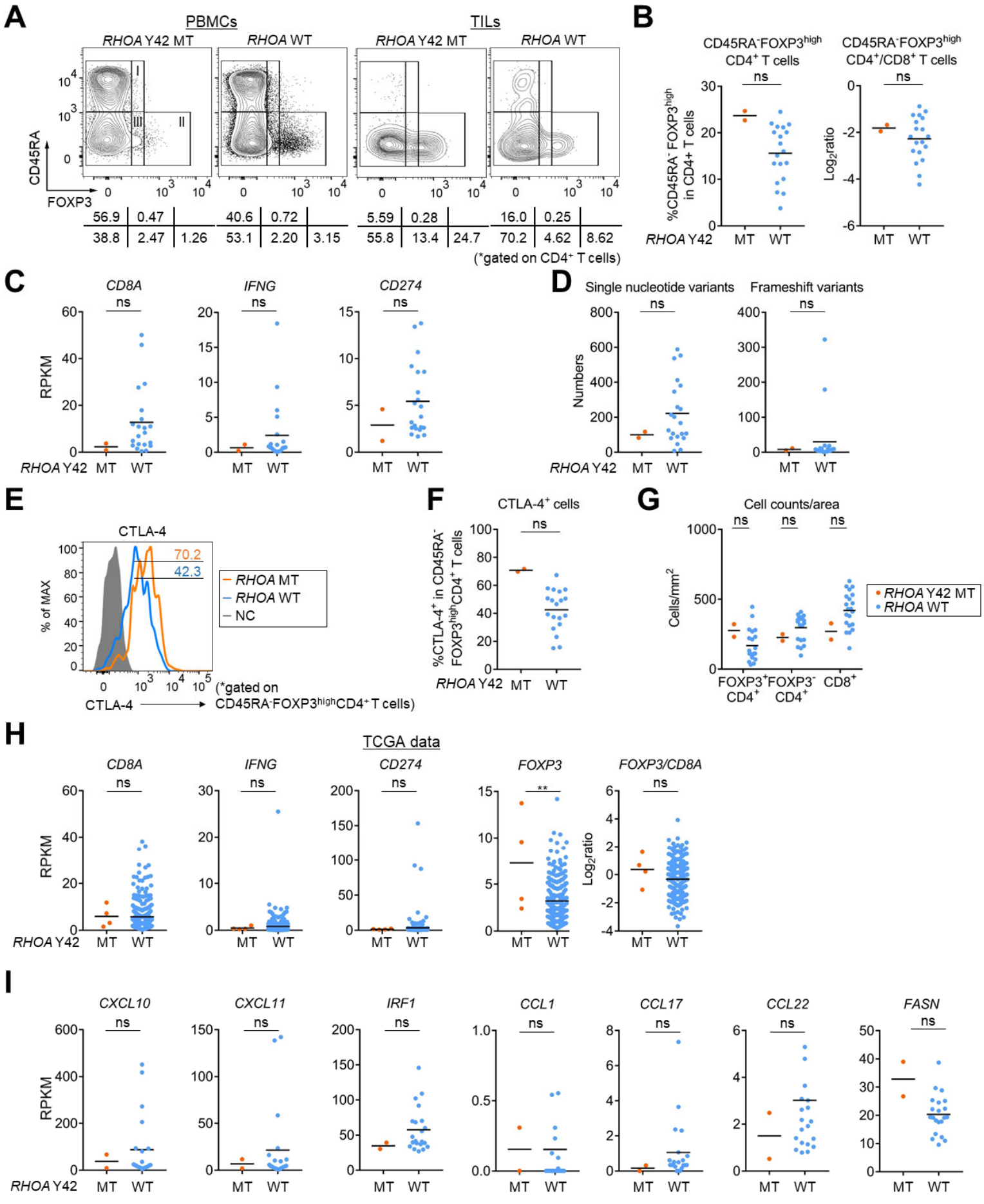
A
PBMCs
TILs
RHOA Y42 MT
RHOA WT
RHOA Y42 MT
RHOA WT
CD45RA
FOXP3
I
II
III
56.9 0.47
38.8 2.47 1.26
40.6 0.72
53.1 2.20 3.15
5.59 0.28
55.8 13.4 24.7
16.0 0.25
70.2 4.62 8.62
(*gated on CD4+ T cells)
B
CD45RA-FOXP3high CD4+ T cells
CD45RA-FOXP3high CD4+/CD8+ T cells
ns
%CD45RA- FOXP3high in CD4+ T cells
Log2ratio
RHOA Y42 MT WT
C
CD8A
IFNG
CD274
ns
RPKM
RHOA Y42 MT WT
D
Single nucleotide variants
Frameshift variants
ns
Numbers
RHOA Y42 MT WT
E
CTLA-4
70.2
42.3
% of MAX
RHOA MT
RHOA WT
NC
CTLA-4
(*gated on CD45RA-FOXP3highCD4+ T cells)
F
CTLA-4+ cells
ns
%CTLA-4+ in CD45RA- FOXP3highCD4+ T cells
RHOA Y42 MT WT
G
Cell counts/area
ns
Cells/mm2
FOXP3+ CD4+
FOXP3- CD4+
CD8+
RHOA Y42 MT
RHOA WT
H
TCGA data
CD8A
IFNG
CD274
FOXP3
FOXP3/CD8A
ns
**
RPKM
Log2ratio
RHOA Y42 MT WT
I
CXCL10
CXCL11
IRF1
CCL1
CCL17
CCL22
FASN
ns
RPKM
RHOA Y42 MT WT

Figure S1

Figure S1. Related to Figure 1. Immune-related gene expression and TMB are not highly detected in *RHOA* Y42-mutated GCs.

(A and B) Representative contour plots of eTreg cells in surgically-resected GC samples classified according to *RHOA* gene status **(A)** and summaries **(B)** are shown. $FOXP3^+$ cells among $CD45RA^-CD4^+$ T cells were defined: the line delineating $FOXP3^+$ cells derived from naive Treg cells demarcated FOXP3 high (eTreg cells) and low (non-Treg cells) in $CD45RA^-CD4^+$ T cells. **(C)** Gene expression of *CD8A*, *IFNG*, and *CD274* was compared according to *RHOA* gene status with RNA-seq data. **(D)** Single nucleotide variants and frameshift variants were assessed according to *RHOA* gene status with WES data. **(E and F)** Representative histogram plots of CTLA-4 expression by eTreg cells in the TME in surgically-resected GC samples classified according to *RHOA* gene status **(E)** and summary of the proportion of $CTLA\text{-}4^+$ cells in eTreg cells **(F)** are shown. **(G)** Summaries of multiplexed IHC for CD4, CD8, and FOXP3-expressing cells according to *RHOA* gene status are shown. **(H)** Gene expression of *CD8A, IFNG, CD274*, and *FOXP3* and the ratio of *FOXP3* to *CD8A* expression were compared according to *RHOA* gene status with RNA-seq data from TCGA data. **(I)** Gene expression of *CXCL10*, *CXCL11*, *IRF1*, *CCL1*, *CCL17*, *CCL22*, and *FASN* was compared according to *RHOA* gene status with RNA-seq data. **, $P < 0.01$; and ns, not significant.

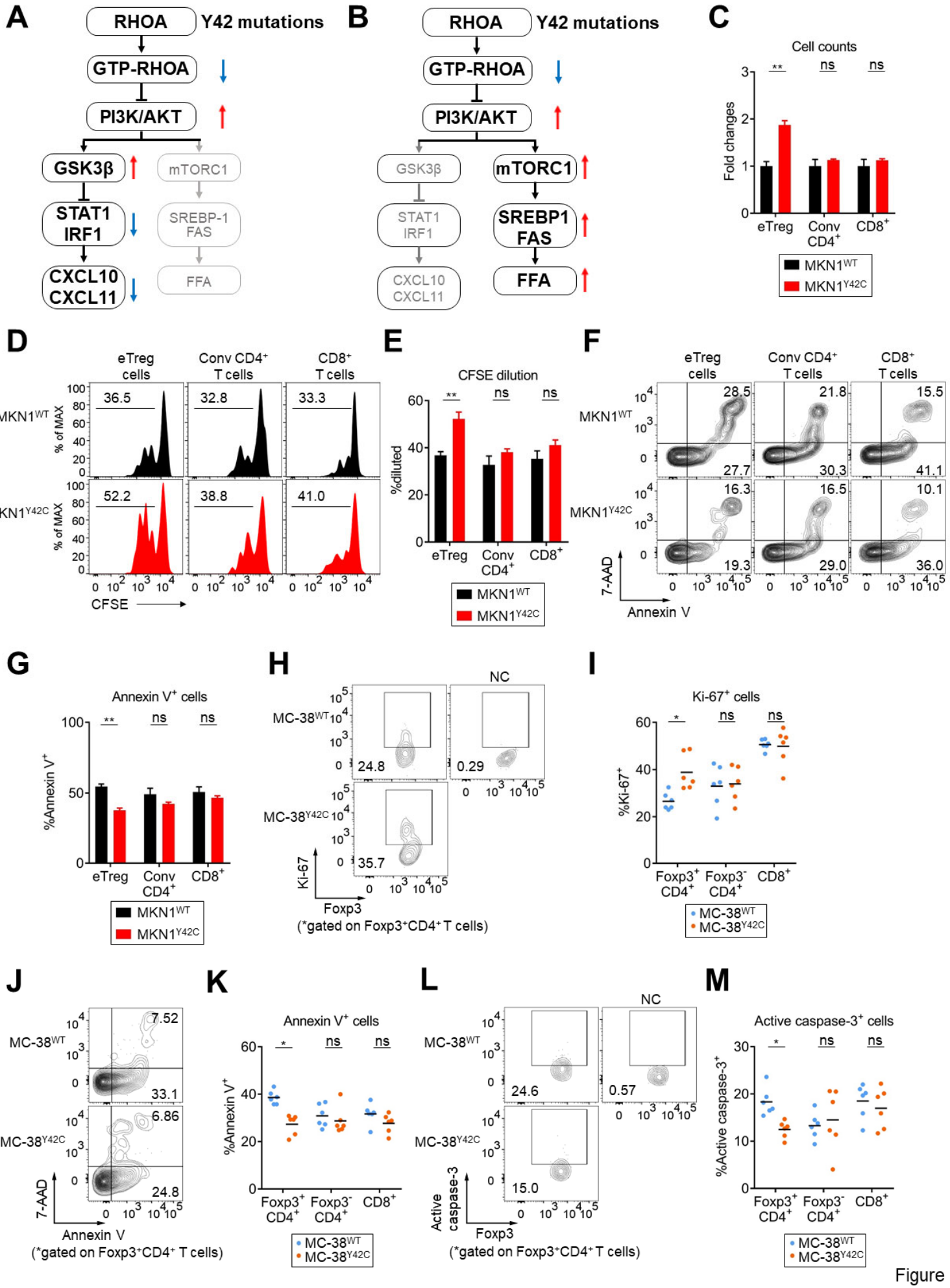
A
RHOA
Y42 mutations
GTP-RHOA
PI3K/AKT
GSK3β
mTORC1
STAT1
IRF1
SREBP-1
FAS
CXCL10
CXCL11
FFA
B
RHOA
Y42 mutations
GTP-RHOA
PI3K/AKT
GSK3β
mTORC1
STAT1
IRF1
SREBP1
FAS
CXCL10
CXCL11
FFA
C
Cell counts
Fold changes
eTreg
Conv CD4+
CD8+
MKN1WT
MKN1Y42C
D
eTreg cells
Conv CD4+ T cells
CD8+ T cells
MKN1WT
MKN1Y42C
% of MAX
36.5
32.8
33.3
52.2
38.8
41.0
CFSE
E
CFSE dilution
%diluted
eTreg
Conv CD4+
CD8+
MKN1WT
MKN1Y42C
F
eTreg cells
Conv CD4+ T cells
CD8+ T cells
MKN1WT
MKN1Y42C
28.5
21.8
15.5
27.7
30.3
41.1
16.3
16.5
10.1
19.3
29.0
36.0
7-AAD
Annexin V
G
Annexin V+ cells
%Annexin V+
eTreg
Conv CD4+
CD8+
MKN1WT
MKN1Y42C
H
NC
MC-38WT
MC-38Y42C
24.8
0.29
35.7
Ki-67
Foxp3
(*gated on Foxp3+CD4+ T cells)
I
Ki-67+ cells
%Ki-67+
Foxp3+ CD4+
Foxp3- CD4+
CD8+
MC-38WT
MC-38Y42C
J
MC-38WT
MC-38Y42C
7.52
33.1
6.86
24.8
7-AAD
Annexin V
(*gated on Foxp3+CD4+ T cells)
K
Annexin V+ cells
%Annexin V+
Foxp3+ CD4+
Foxp3- CD4+
CD8+
MC-38WT
MC-38Y42C
L
NC
MC-38WT
MC-38Y42C
24.6
0.57
15.0
Active caspase-3
Foxp3
(*gated on Foxp3+CD4+ T cells)
M
Active caspase-3+ cells
%Active caspase-3+
Foxp3+ CD4+
Foxp3- CD4+
CD8+
MC-38WT
MC-38Y42C

Figure S2

Figure S2. Related to Figure 5. *RHOA* Y42 mutations promote the survival of eTreg cells *in vitro* and *in vivo*.

(A and B) Schemas of signaling pathways in cancer cells harboring *RHOA* Y42 mutations. The changes of signaling pathways for gene expression of CXCL10, CXCL11, and IRF1 **(A)** and SREBP-1, FAS, and FFA **(B)** are shown. **(C-G)** $MKN1^{WT}$ or $MKN1^{Y42C}$ cells were cultured for seven days in glucose-free RPMI medium supplemented with 10% lipid-without FBS under low-glucose (3mM) condition. eTreg cells, conv $CD4^+$ T cells, and $CD8^+$ T cells were sorted from PBMCs of healthy individuals. Each T cell subset stimulated with anti-CD3 mAb and anti-CD28 mAb was cultured with irradiated APCs in the same wells of $MKN1^{WT}$ or $MKN1^{Y42C}$ cells without contact with cancer cells. **(C)** After ninety-six-hour incubation, cell counts of indicated T cell subsets were calculated with FCM. Cell counts of each T cell subset cultured with $MKN1^{WT}$ or $MKN1^{Y42C}$ are shown. **(D and E)** After ninety-six-hour incubation, proliferation was assessed by dilution of CFSE-labelled cells with FCM. Representative histograms of CFSE dilution **(D)** and summaries **(E)** are shown. **(F and G)** After forty-eight-hour incubation, apoptosis was evaluated by Annexin V and 7-AAD staining. Representative contour plots of Annexin V and 7-AAD **(F)** and summaries **(G)** are shown. **(H-M)** $MC\text{-}38^{WT}$ or $MC\text{-}38^{Y42C}$ cells (1.0×10^6) were injected subcutaneously into *Foxp3*$^{Thy1.1}$ C57BL/6 mice on day 0 (N = 6). TILs prepared from tumor tissue samples on day 12 were subjected to FCM. Apoptosis was evaluated by Annexin V and 7-AAD staining and by assessing active caspase-3^+ T cells. Proliferation was detected by Ki-67 staining. Representative contour plots **(H, J, and L)** and summaries **(I, K, and M)** are shown **(H and I**, Foxp3 and Ki-67; **J and K,** Annexin V and 7-AAD; and **L and M**, Foxp3 and active caspase-3**)**. Means from three independent experiments are shown. NC, negative control; Bars, mean; error bars, SEM; *, $P < 0.05$; **, $P < 0.01$; and ns, not significant.

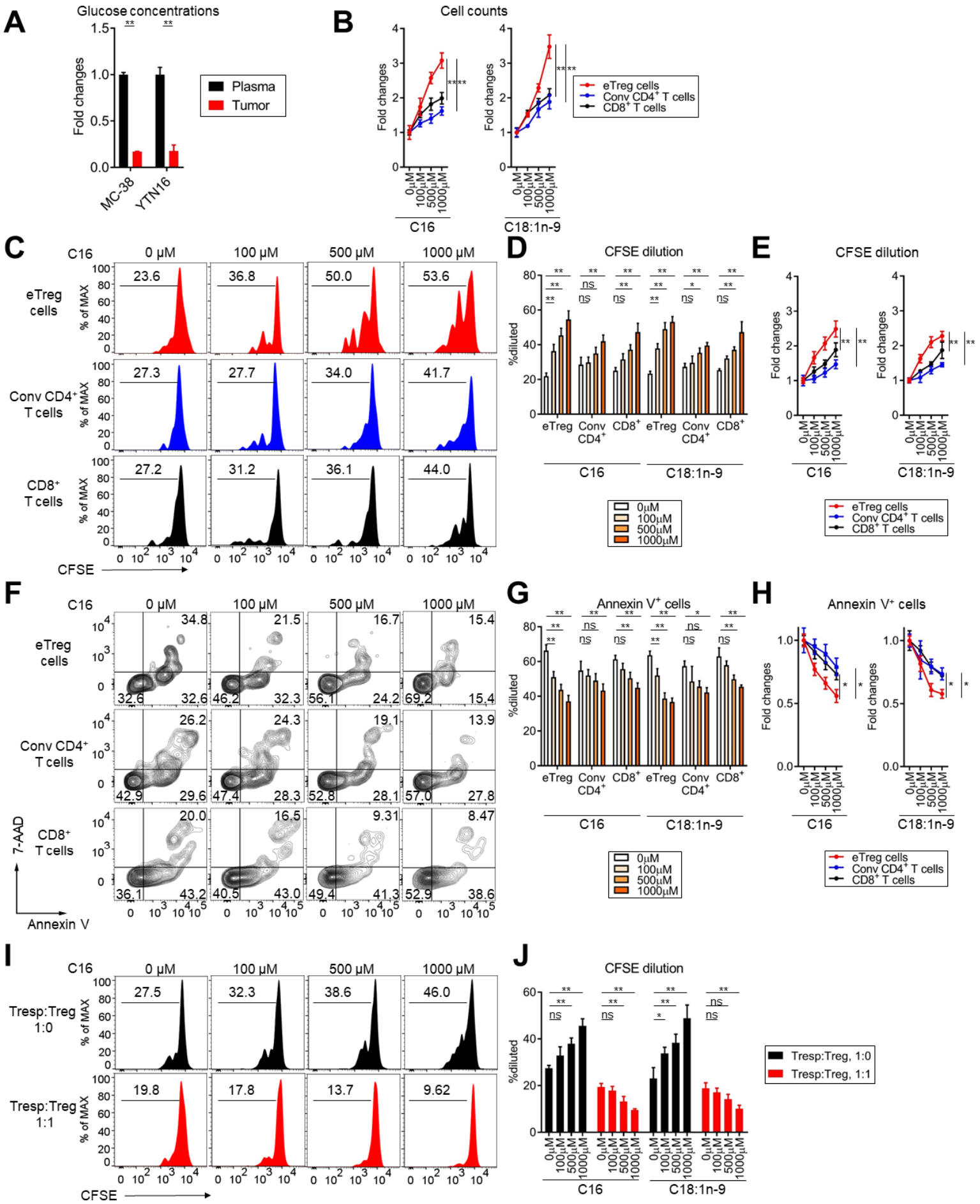
A
Glucose concentrations
Fold changes
Plasma
Tumor
MC-38
YTN16
B
Cell counts
Fold changes
eTreg cells
Conv CD4+ T cells
CD8+ T cells
0μM
100μM
500μM
1000μM
C16
C18:1n-9
C
C16
0 μM
100 μM
500 μM
1000 μM
eTreg cells
Conv CD4+ T cells
CD8+ T cells
% of MAX
CFSE
D
CFSE dilution
%diluted
eTreg
Conv CD4+
CD8+
E
CFSE dilution
F
7-AAD
Annexin V
G
Annexin V+ cells
H
Annexin V+ cells
I
Tresp:Treg 1:0
Tresp:Treg 1:1
J
CFSE dilution
Tresp:Treg, 1:0
Tresp:Treg, 1:1

Figure S3

Figure S3. Related to Figure 3. eTreg cells efficiently survive compared to other T cell subsets under low-glucose condition in an FFA dose dependent manner.

(A) MC-38 or YTN16 cells (1.0×10^6) were injected subcutaneously into C57BL/6 mice on day 0 (N = 4). On day 12, plasma and tumor fluids were extracted from blood and tumors, respectively. Glucose concentrations in plasma and tumor fluids were evaluated with the Glucose Assay Kit. **(B-H)** eTreg cells, conv $CD4^+$ T cells, and $CD8^+$ T cells were sorted from PBMCs of healthy individuals. Each T cell subset stimulated by anti-CD3 mAb and anti-CD28 mAb was cultured with irradiated APCs in glucose-free RPMI medium supplemented with 10% lipid-without FBS under low-glucose (1 mM) condition and the indicated concentration of palmitate-BSA or oleate-BSA. **(B-E)** After ninety-six-hour incubation, cell counts or proliferation of the indicated T cell subsets were evaluated with FCM. Proliferation was assessed by dilution of CFSE-labelled cells. Representative histograms of CFSE dilution **(C)** and summaries of cell counts **(B)** or CFSE dilution **(D and E)** are shown. **(F-H)** After forty-eight-hour incubation, apoptosis was evaluated by Annexin V and 7-AAD staining. Representative contour plots for Annexin V and 7-AAD **(F)** and summaries **(G and H)** are shown. **(I and J)** CFSE-labelled responder $CD8^+$ T cells sorted from PBMCs of healthy individuals were cocultured with or without unlabeled eTreg cells and stimulated with anti-CD3 mAb in glucose-free RPMI medium supplemented with 10% lipid-without FBS under low-glucose (1 mM) condition and the indicated concentration of palmitate-BSA or oleate-BSA. After ninety-six hours, proliferation was assessed by dilution of CFSE-labelled cells with FCM. Representative histograms of CFSE dilution **(I)** and summaries of suppressive function **(J)** are shown. Means from three independent experiments are shown. Bars, mean; error bars, SEM; *, $P<0.05$; **, $P < 0.01$; and ns, not significant.

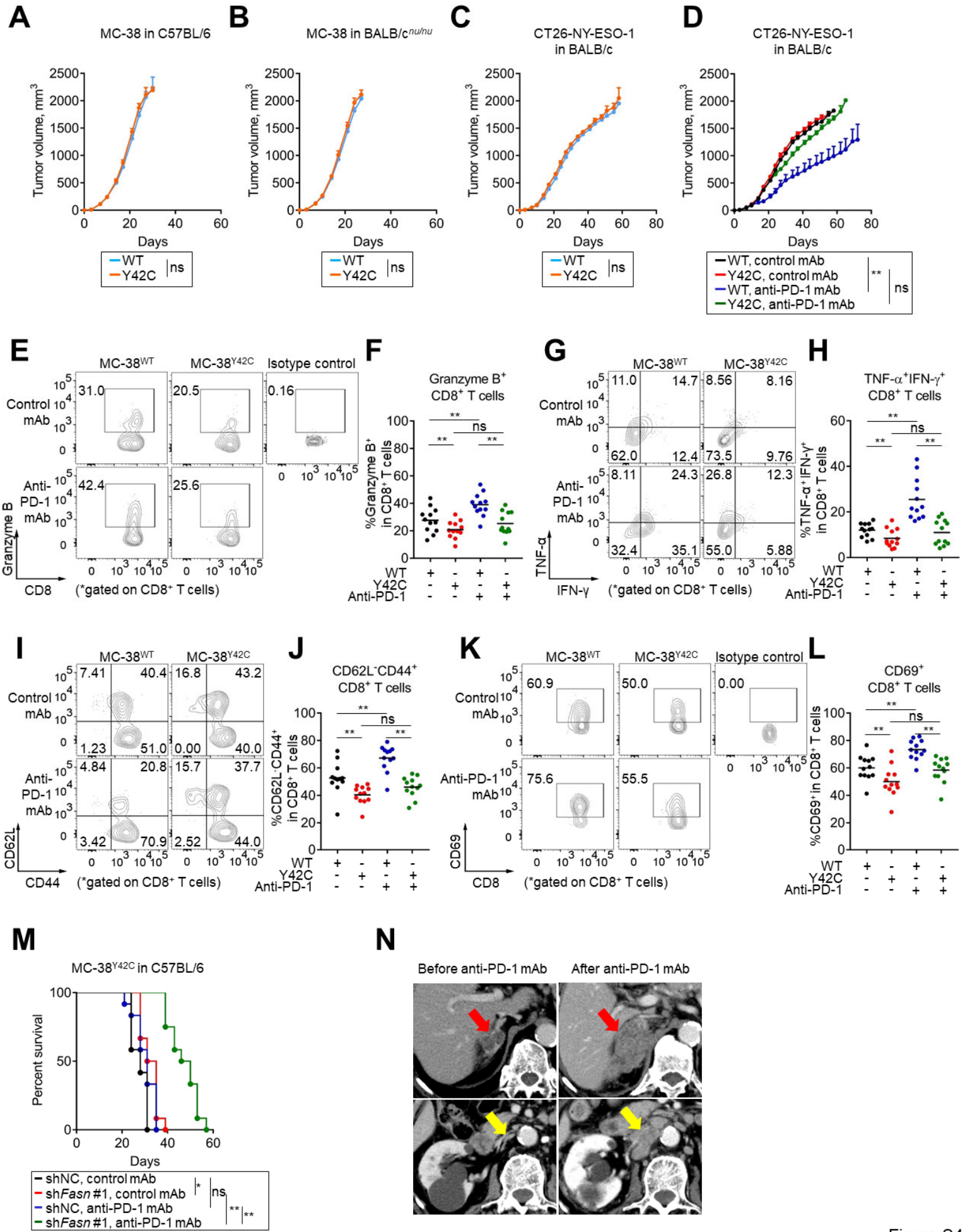
A
MC-38 in C57BL/6
Tumor volume, mm3
Days
WT
Y42C
ns
B
MC-38 in BALB/cnu/nu
C
CT26-NY-ESO-1 in BALB/c
D
CT26-NY-ESO-1 in BALB/c
WT, control mAb
Y42C, control mAb
WT, anti-PD-1 mAb
Y42C, anti-PD-1 mAb
**
E
MC-38WT
MC-38Y42C
Isotype control
Control mAb
Anti-PD-1 mAb
31.0
20.5
0.16
42.4
25.6
Granzyme B
CD8
(*gated on CD8+ T cells)
F
Granzyme B+ CD8+ T cells
%Granzyme B+ in CD8+ T cells
WT
Y42C
Anti-PD-1
G
11.0
14.7
8.56
8.16
62.0
12.4
73.5
9.76
8.11
24.3
26.8
12.3
32.4
35.1
55.0
5.88
TNF-α
IFN-γ
H
TNF-α+IFN-γ+ CD8+ T cells
%TNF-α+IFN-γ+ in CD8+ T cells
I
7.41
40.4
16.8
43.2
1.23
51.0
0.00
40.0
4.84
20.8
15.7
37.7
3.42
70.9
2.52
44.0
CD62L
CD44
J
CD62L-CD44+ CD8+ T cells
%CD62L-CD44+ in CD8+ T cells
K
60.9
50.0
0.00
75.6
55.5
CD69
CD8
L
CD69+ CD8+ T cells
%CD69+ in CD8+ T cells
M
MC-38Y42C in C57BL/6
Percent survival
shNC, control mAb
shFasn #1, control mAb
shNC, anti-PD-1 mAb
shFasn #1, anti-PD-1 mAb
*
**
N
Before anti-PD-1 mAb
After anti-PD-1 mAb

Figure S4

Figure S4. Related to Figure 5 and 6. Tumor growth is comparable according to *RHOA* gene status and *RHOA* Y42 mutations significantly change the immunological status of the TME.

(A) MC-38^{WT} or MC-38^{Y42C} cells (1.0×10^6) were injected subcutaneously into immunocompetent wild-type C57BL/6 mice on day 0 (N = 12 per group). **(B)** MC-38^{WT} or MC-38^{Y42C} cells (1.0×10^6) were injected subcutaneously into immunocompromised BALB/c$^{nu/nu}$ mice on day 0 (N = 12 per group). **(C)** CT26-NY-ESO-1^{WT} or CT26-NY-ESO-1^{Y42C} cells (1.0×10^6) were injected subcutaneously into BALB/c mice on day 0 (N = 12 per group). **(D)** CT26-NY-ESO-1^{WT} or CT26-NY-ESO-1^{Y42C} cells (1.0×10^6) were injected subcutaneously into BALB/c mice on day 0, and anti-PD-1 mAb was administered on days 6, 11, and 16 (N = 12 per group). **(E-L)** MC-38^{WT} or MC-38^{Y42C} cells (1.0×10^6) were injected subcutaneously into C57BL/6 mice on day 0, and anti-PD-1 mAb was administered on days 6, 11, and 16 (N = 12 per group). TILs prepared from tumor tissue samples on day 12 were subjected to FCM. Representative contour plots (**E, G, I, and K**) and summaries **(F, H, J, and L)** (N = 12) of FCM analysis are shown **(E and F,** CD8 and Granzyme B; **G and H,** IFN-γ and TNF-α; **I and J,** CD44 and CD62L; and **K and L,** CD8 and CD69**)**. **(M)** MC-38^{Y42C}-shNC or MC-38^{Y42C}-sh*Fasn* cells (1.0×10^6) were injected subcutaneously into C57BL/6 mice on day 0, and anti-PD-1 mAb or control mAb was administered on days 6, 11, and 16 (N = 12 per group). Survival curves of the indicated groups are shown. **(N)** An 82-year-old male patient with advanced diffuse-type *RHOA*-mutated gastric cancer with multiple metastases to the lymph nodes, peritoneum and adrenal gland. The patient received third-line anti-PD-1 mAb therapy. An initial evaluation with computed tomography (CT) after anti-PD-1 mAb administration showed progressive disease. Representative CT images before (left top and bottom) and after one course of anti-PD-1 mAb therapy (right top and bottom) are shown. The metastasis lesions of the right adrenal gland and of paraaortic lymph nodes were enlarged. Red and yellow arrows indicate the metastasis lesions of the right adrenal gland and of paraaortic lymph nodes, respectively. NC, negative control; *, $P<0.05$; **, $P < 0.01$; and ns, not significant.

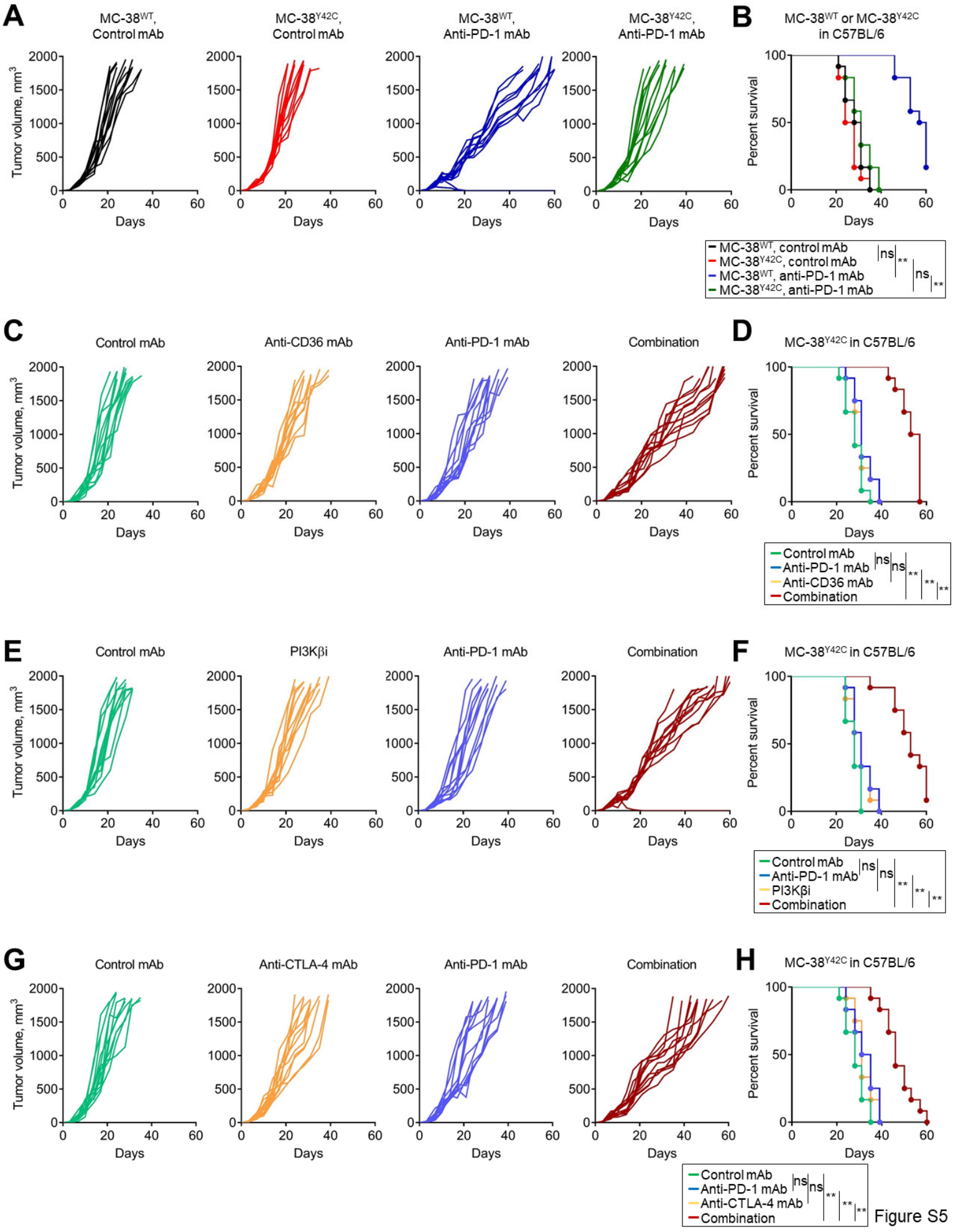
A
MC-38WT, Control mAb
MC-38Y42C, Control mAb
MC-38WT, Anti-PD-1 mAb
MC-38Y42C, Anti-PD-1 mAb
Tumor volume, mm3
Days
B
MC-38WT or MC-38Y42C in C57BL/6
Percent survival
MC-38WT, control mAb
MC-38Y42C, control mAb
MC-38WT, anti-PD-1 mAb
MC-38Y42C, anti-PD-1 mAb
ns
**
C
Control mAb
Anti-CD36 mAb
Anti-PD-1 mAb
Combination
D
MC-38Y42C in C57BL/6
Control mAb
Anti-PD-1 mAb
Anti-CD36 mAb
Combination
E
PI3Kβi
F
MC-38Y42C in C57BL/6
G
Anti-CTLA-4 mAb
H
MC-38Y42C in C57BL/6

Figure S5

Figure S5. Related to Figure 6 and 7. *RHOA* Y42-mutated tumors are resistant to anti-PD-1 mAb and responsive to combination of anti-CD36 mAb, PI3Kβi or anti-CTLA-4 mAb with anti-PD-1 mAb.

(A and B) MC-38^{WT} or MC-38^{Y42C} cells (1.0×10^6) were injected subcutaneously into C57BL/6 mice on day 0, and anti-PD-1 mAb was administered on days 6, 11, and 16 (N = 12 per group). Individual tumor growth curves **(A)** and survival curves **(B)** are shown. **(C and D)** MC-38^{Y42C} cells (1.0×10^6) were injected subcutaneously into C57BL/6 mice on day 0, and anti-PD-1 mAb (intravenously, on days 6, 11, and 16) or anti-CD36 mAb (intravenously, daily) was administered (N = 12 per group). Individual tumor growth curves **(C)** and survival curves **(D)** are shown. **(E and F)** MC-38^{Y42C} cells (1.0×10^6) were injected subcutaneously into C57BL/6 mice on day 0. The mice were treated with anti-PD-1 mAb (intravenously, on days 6, 11, and 16) and/or GSK2636771 (orally, for five days) (N = 12 per group). Individual tumor growth curves **(E)** and survival curves **(F)** are shown. **(G and H)** MC-38^{Y42C} cells (1.0×10^6) were injected subcutaneously into C57BL/6 mice on day 0. These mice were treated with anti-PD-1 mAb (intravenously, on days 6, 11, and 16) and/or anti-CTLA-4 mAb (intravenously, on days 6, 11, and 16) (N = 12 per group). Individual tumor growth curves **(G)** and survival curves **(H)** are shown. Bars, mean; error bars, SEM; **, $P < 0.01$; and ns, not significant.

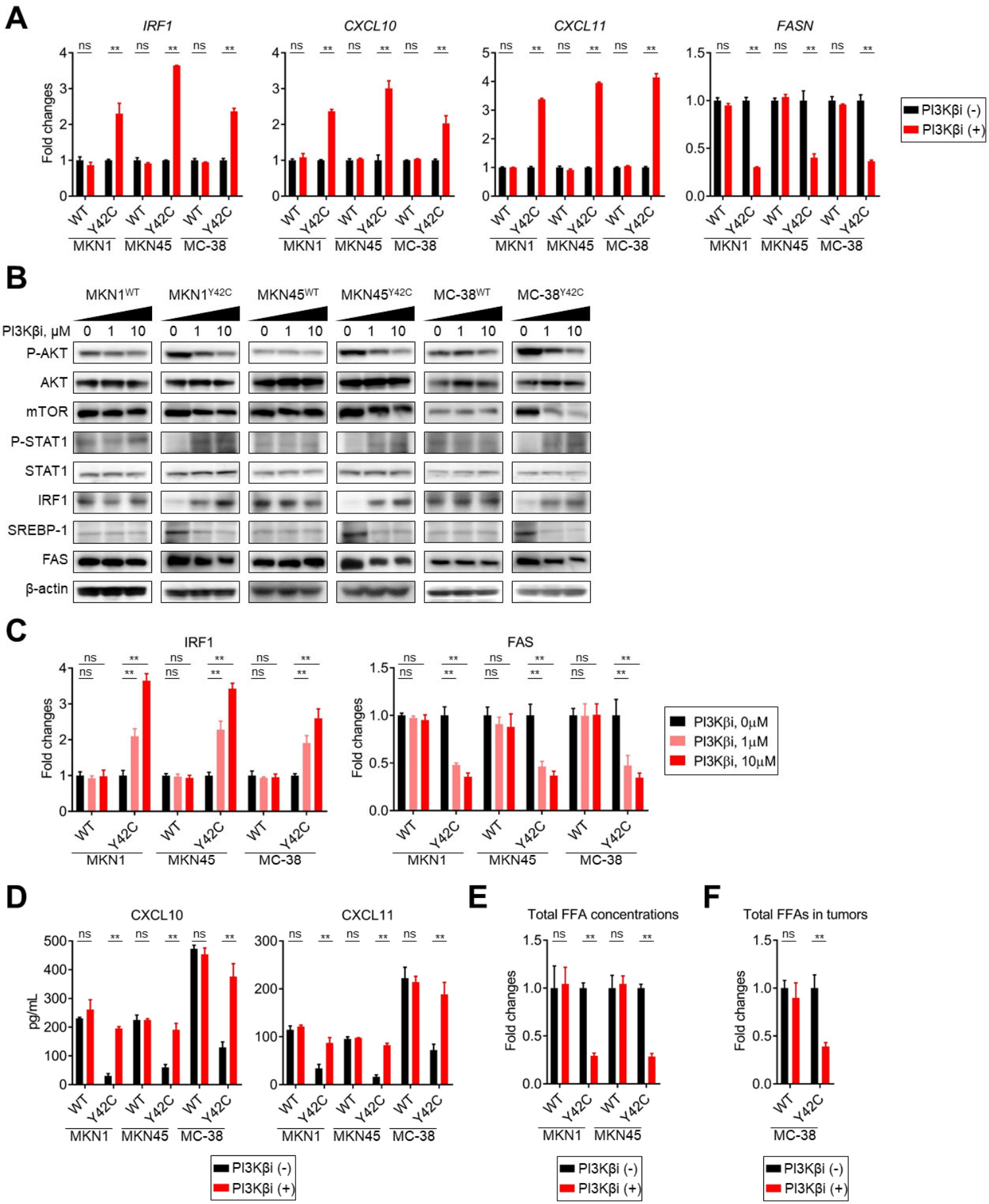
A
IRF1
CXCL10
CXCL11
FASN
Fold changes
ns
**
WT
Y42C
MKN1
MKN45
MC-38
PI3Kβi (-)
PI3Kβi (+)
B
MKN1WT
MKN1Y42C
MKN45WT
MKN45Y42C
MC-38WT
MC-38Y42C
PI3Kβi, μM 0 1 10
P-AKT
AKT
mTOR
P-STAT1
STAT1
IRF1
SREBP-1
FAS
β-actin
C
IRF1
FAS
Fold changes
PI3Kβi, 0μM
PI3Kβi, 1μM
PI3Kβi, 10μM
D
CXCL10
CXCL11
pg/mL
PI3Kβi (-)
PI3Kβi (+)
E
Total FFA concentrations
F
Total FFAs in tumors

Figure S6

Figure S6. Related to Figure 7. A PI3Kβ inhibitor increases the levels of effector T cell-recruiting chemokines and reduces the levels of FFAs by inhibiting the PI3K-AKT signaling pathways in *RHOA* Y42C-overexpressing cell lines.

(A) *RHOA*-overexpressing cell lines were treated with 10 μM GSK2636771 for 24 hours. The expression of *IRF1*, *CXCL10*, *CXCL11*, and *FASN* was examined with real-time qRT-PCR. Fold changes relative to each cell line treated with DMSO are shown. **(B and C)** *RHOA*-overexpressing cell lines were treated with titrated doses (0, 1, and 10 μM) of GSK2636771 for 24 hours, and the indicated protein expression was examined by western blotting (**B**). Summaries of quantified IRF1 (IRF1/β-actin) and FAS (FAS/β-actin) expression in the GSK2636771-treated cell lines relative to the expression in each cell line treated with DMSO are shown (**C**). **(D and E)** *RHOA*-overexpressing cell lines were treated with 10 μM GSK2636771 for 24 hours. **(D)** The concentrations of CXCL10 and CXCL11 in the culture medium of *RHOA* WT- or *RHOA* Y42C-overexpressing cell lines were analyzed with ELISA. **(E)** The total FFA concentration in the culture medium of *RHOA* WT or Y42C-overexpressing cell lines was assessed with the Free Fatty Acid Quantification Kit. Fold changes relative to each cell line treated with DMSO are shown. **(F)** MC-38^{WT} or MC-38^{Y42C} cells (1.0×10^6) were injected subcutaneously into C57BL/6 mice on day 0, and GSK2636771 was administered orally for five days (N = 3 per group). Tumor interstitial fluids were extracted from the MC-37^{WT} or MC-38^{Y42C} tumors on day 12. Total FFAs in the interstitial fluids of the MC-38^{WT} or MC-38^{Y42C} tumors were evaluated by the Free Fatty Acid Quantification Kit. β-actin and *18S* ribosomal RNA were used as internal controls for protein and mRNA expression analyses, respectively. Means from three independent experiments are presented. Bars, mean; error bars, SEM; PI3Kβi, PI3Kβ inhibitor; **, $P < 0.01$; and ns, not significant.

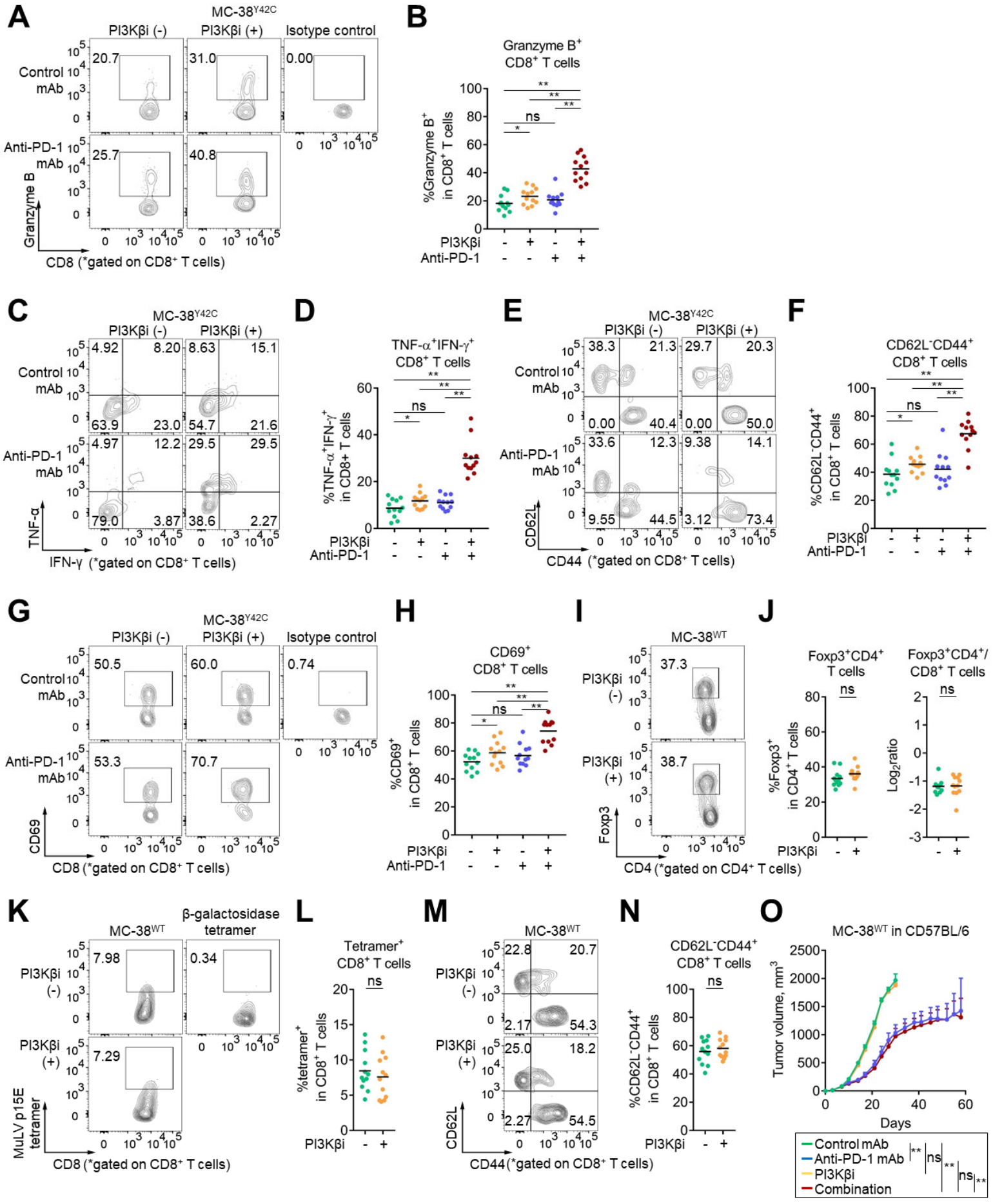
A
MC-38Y42C
PI3Kβi (-)
PI3Kβi (+)
Isotype control
Control mAb
Anti-PD-1 mAb
20.7
31.0
0.00
25.7
40.8
Granzyme B
CD8 (*gated on CD8+ T cells)
B
Granzyme B+ CD8+ T cells
%Granzyme B+ in CD8+ T cells
ns
PI3Kβi
Anti-PD-1
C
MC-38Y42C
4.92
8.20
8.63
15.1
63.9
23.0
54.7
21.6
4.97
12.2
29.5
29.5
79.0
3.87
38.6
2.27
TNF-α
IFN-γ (*gated on CD8+ T cells)
D
TNF-α+IFN-γ+ CD8+ T cells
%TNF-α+IFN-γ+ in CD8+ T cells
E
MC-38Y42C
38.3
21.3
29.7
20.3
0.00
40.4
0.00
50.0
33.6
12.3
9.38
14.1
9.55
44.5
3.12
73.4
CD62L
CD44 (*gated on CD8+ T cells)
F
CD62L-CD44+ CD8+ T cells
%CD62L-CD44+ in CD8+ T cells
G
MC-38Y42C
50.5
60.0
0.74
53.3
70.7
CD69
CD8 (*gated on CD8+ T cells)
H
CD69+ CD8+ T cells
%CD69+ in CD8+ T cells
I
MC-38WT
37.3
38.7
Foxp3
CD4 (*gated on CD4+ T cells)
J
Foxp3+CD4+ T cells
%Foxp3+ in CD4+ T cells
Foxp3+CD4+/ CD8+ T cells
Log2ratio
K
MC-38WT
β-galactosidase tetramer
7.98
0.34
7.29
MuLV p15E tetramer
CD8 (*gated on CD8+ T cells)
L
Tetramer+ CD8+ T cells
%tetramer+ in CD8+ T cells
M
MC-38WT
22.8
20.7
2.17
54.3
25.0
18.2
2.27
54.5
CD44 (*gated on CD8+ T cells)
N
CD62L-CD44+ CD8+ T cells
%CD62L-CD44+ in CD8+ T cells
O
MC-38WT in CD57BL/6
Tumor volume, mm3
Days
Control mAb
Anti-PD-1 mAb
PI3Kβi
Combination

Figure S7

Figure S7 Related to Figure 7. The combination of PI3Kβ inhibitor and anti-PD-1 mAb improves the immunological status of the TME of MC-38^{Y42C} tumors, but not MC-38^{WT} tumors.

(A-I) MC-38^{Y42C} cells (1.0×10^6) were injected subcutaneously into C57BL/6 mice on day 0. The mice were treated with anti-PD-1 mAb (intravenously, on days 6 and 11) and/or GSK2636771 (orally, for five days) (N = 12 per group). TILs prepared from tumor tissue samples on day 12 were subjected to FCM. Tumor growth was monitored twice weekly. Representative contour plots **(A, C, E and G)** and summaries **(B, D, F and H)** (N = 12) are shown **(A and B,** CD8 and Granzyme B; **C and D,** and IFN-γ and TNF-α; **E and F,** CD44 and CD62L; and **G and H,** CD8 and CD69**)**. **(I-O)** MC-38^{WT} cells (1.0×10^6) were injected subcutaneously into C57BL/6 mice on day 0, and GSK2636771 was administered orally for five days (N=12 per group). TILs prepared from tumor tissue samples on day 12 were subjected to FCM. The frequency of Treg cells in the TME was evaluated. MC-38 tumor antigen-specific $CD8^+$ T cells detected by MuLV p15E/H-2Kb tetramers and the activation of $CD8^+$ T cells in the TME were analyzed. Representative contour plots **(I, K, and M)** and summaries **(J, L, and N)** (N = 12) are shown. **(I and J,** CD4 and Foxp3; **K and L,** CD8 and MuLV p15E/H-2Kb tetramer; **M and N,** CD44 and CD62L**)**. **(O)** MC-38^{WT} cells (1.0×10^6) were injected subcutaneously on day 0. The mice were treated with anti-PD-1 mAb (intravenously, on days 6, 11, and 16) and/or GSK2636771 (orally, for five days) (N = 12 per group). Bars, mean; error bars, SEM; PI3Kβi, PI3Kβ inhibitor; *, $P < 0.05$;**, $P < 0.01$; and ns, not significant.

Patient characteristics	N=23
Sex, male/female	16/7
Age, median (range)	73 (54-86)
Histology	
Diffuse	5
Intestinal	18
pT	
T1	4
T2	4
T3	7
T4	8
pN	
N0	11
N1	6
N2	2
N3	4
pM	
M0	21
M1	2
pStage	
I	5
II	11
III	5
IV	2
FCM analysis of TILs	21

Table S1 Related to Figure1. Characteristics of surgically-resected GC patients

Patient characteristics	N=85
Sex, male/female	59/26
Age, median (range)	67 (39-85)
PS	
0/1	22/63
Histology	
Diffuse/Intestinal/Others	57/24/4
PD-L1	
Positive/negative/unknown	12/68/5
EBV status	
Positive/negative/unknown	5/73/7
MMR status	
Proficient/deficient/unknown	73/4/8

PS, ECOG performance status; EBV, Epstein-Barr virus; MMR, mismatch repair

Table S2 Related to Figure 1. Characteristics of advanced GC patients enrolled in immunological analysis.

Patient characteristics	N=7
Sex, male/female	5/2
Age, median (range)	67 (54-80)
PS	
0/1	2/5
Histology	
Diffuse/Intestinal	6/1
PD-L1	
Positive/negative/unknown	0/6/1
EBV status	
Positive/negative/unknown	0/6/1
MMR status	
Proficient/deficient/unknown	6/0/1
BODIPY FL C16 assay	5
BODIPY 493 assay	5

PS, ECOG performance status; EBV, Epstein-Barr virus; MMR, mismatch repair

Table S3 Related to Figure 4. Characteristics of advanced GC patients for BODIPY analysis.

Case	Sex	Age	PS	Histology	Histological subtype	*RHOA* gene mutations	Sites of metastasis	PD-L1 positivity	EBV status	MMR status	Response
#1	Male	82	1	Adenocarcinoma	diffuse	V9G, Y42H	LN, peritoneum, adrenal gland	0%	-	Proficient	PD
#2	Male	59	0	Adenocarcinoma	diffuse	Y42C	LN, peritoneum	0%	-	Proficient	SD
#3	Male	65	1	Adenocarcinoma	diffuse	Y42C	Peritoneum	0%	-	Proficient	PD

PS, ECOG performance status; LN, lymph node; EBV, Epstein-Barr virus; MMR, mismatch repair

Table S4 Related to Figure 6. Characteristics of three advanced GC patients with *RHOA* mutations who received anti-PD-1 mAb